




Supplementary Information

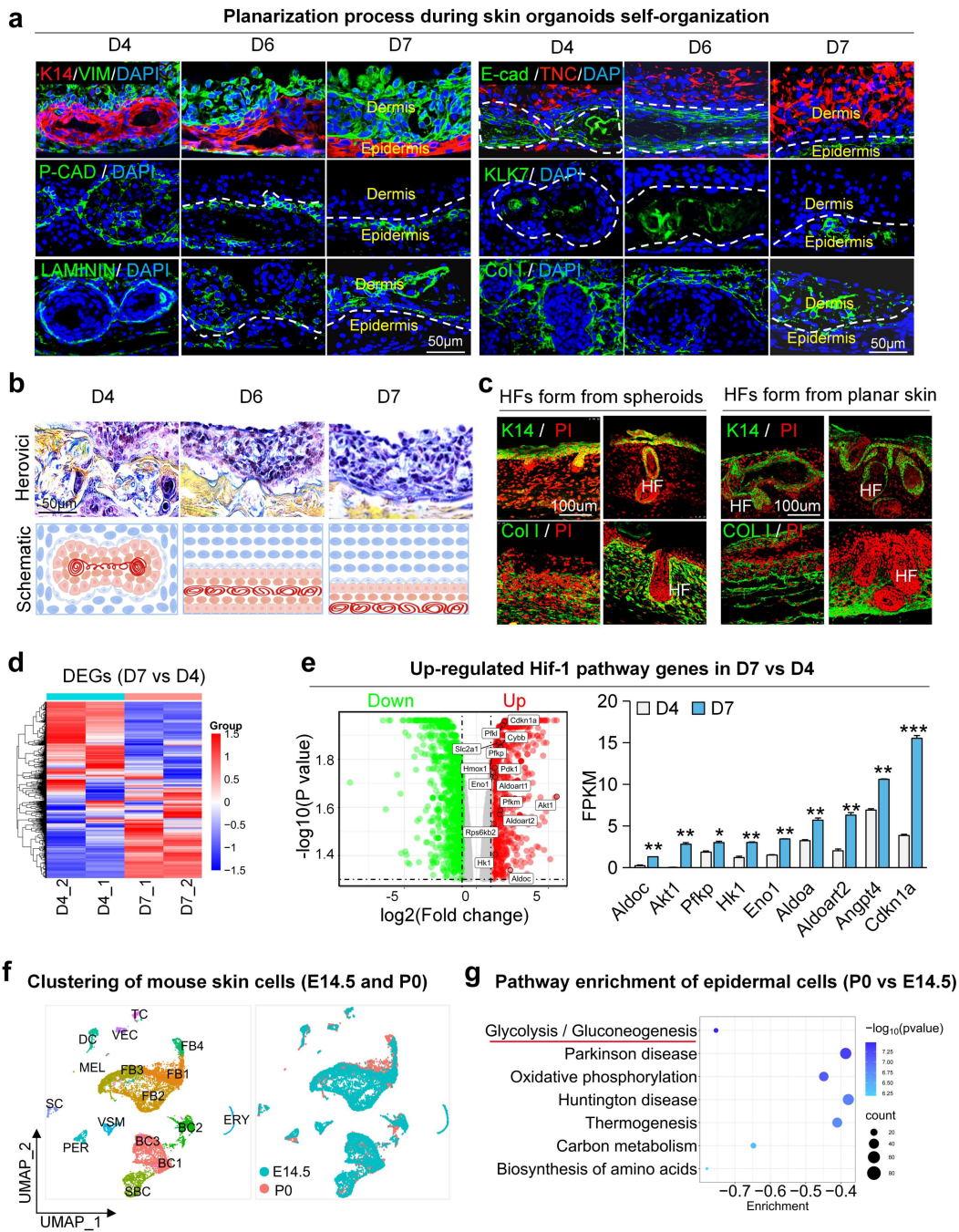
Metabolic adaptation drives self-organization in skin organoid morphogenesis

Jingwei Jiang¹, Weiwei Liu¹, Mengyue Wang¹, Dehuan Wang¹, Wang Wu¹, Man Zhang¹, Siyi Zhou¹, Yang Xiao¹, Weiyi An², Hengguang Zhao², Rixing Zhan³, Li Yang¹, Gaoxing Luo³, Cheng-Ming Chuong⁴, Mingxing Lei¹

This file includes the following subsections:

- **Extended Data Fig. 1-7**
- **Supplementary Table 1-3**

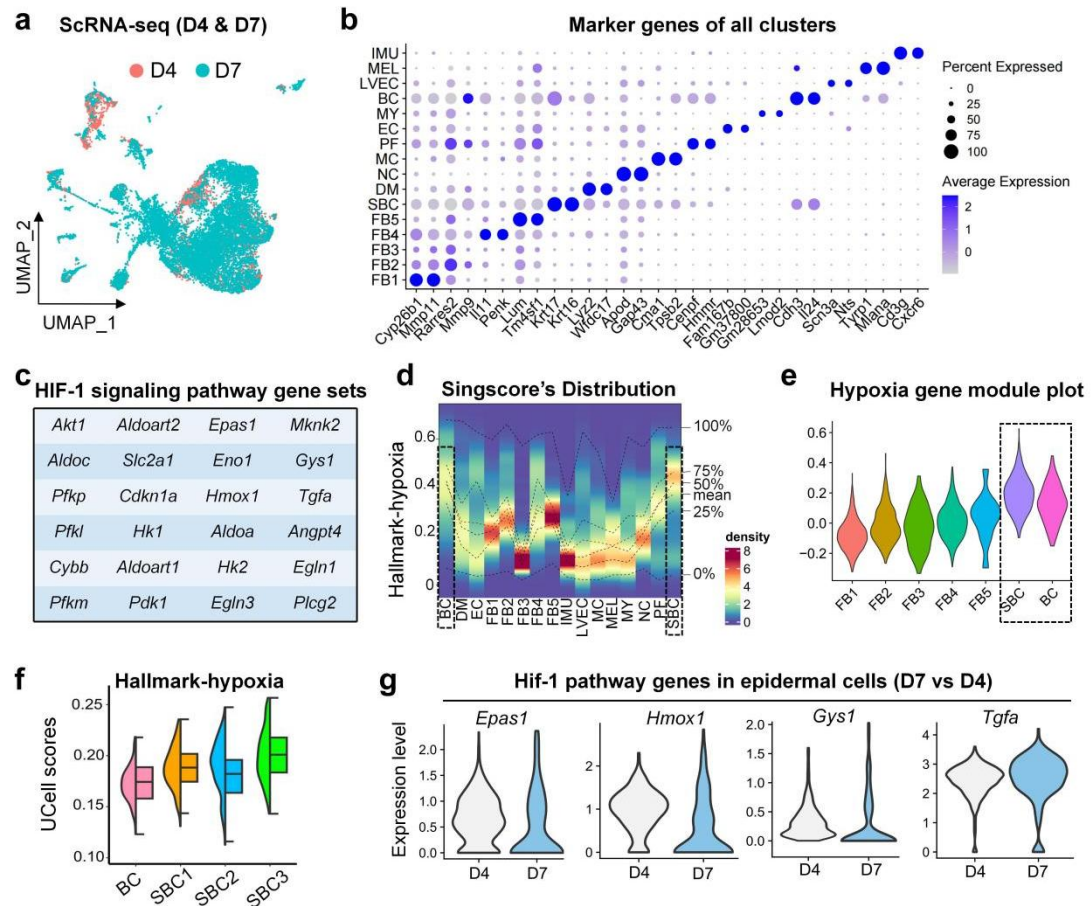
Extended Data Fig. 1



Extended Data Fig. 1: Hypoxia adaptation during skin organoid morphogenesis

- a. Representative immunostaining images to show the transition of skin organoids from coalescence to planarization (D4, D6, D7), as demonstrated by K14 and E-cad for the epidermal cells, Tnc, Vim, and Col I for the pan-fibroblasts, P-cad for the basal cells, Klk7 for the suprabasal cells, Laminin for the basement membrane.
- b. Representative Herovici staining images displaying the dynamic changes of keratin debris and collagen synthesis during self-organization of the skin organoids, newly formed collagen is blue, mature collagen is red, and keratin is yellow. n=3.
- c. Immunofluorescence staining of K14 and Col I reveals the epidermal and dermal structures of cystic hair follicles and planar skin follicles in nude mice after transplantation.
- d. Heatmap displaying the differentially expressed genes (DEGs) between D4 and D7 skin organoids, with 2 replicates per group.
- e. Left: Volcano plot showing the upregulated Hif-1 pathway genes in D7 skin organoids. Right: Bar graph illustrating the upregulated Hif-1 pathway genes in D7 skin organoids, ** $p < 0.01$, *** $p < 0.001$.
- f. UMAP to show the clustering of mouse skin cells (E14.5 and P0).
- g. Bubble plot show the GO enrichment analysis of differentially expressed genes in epidermal cells between P0 skin and E14.5 skin.

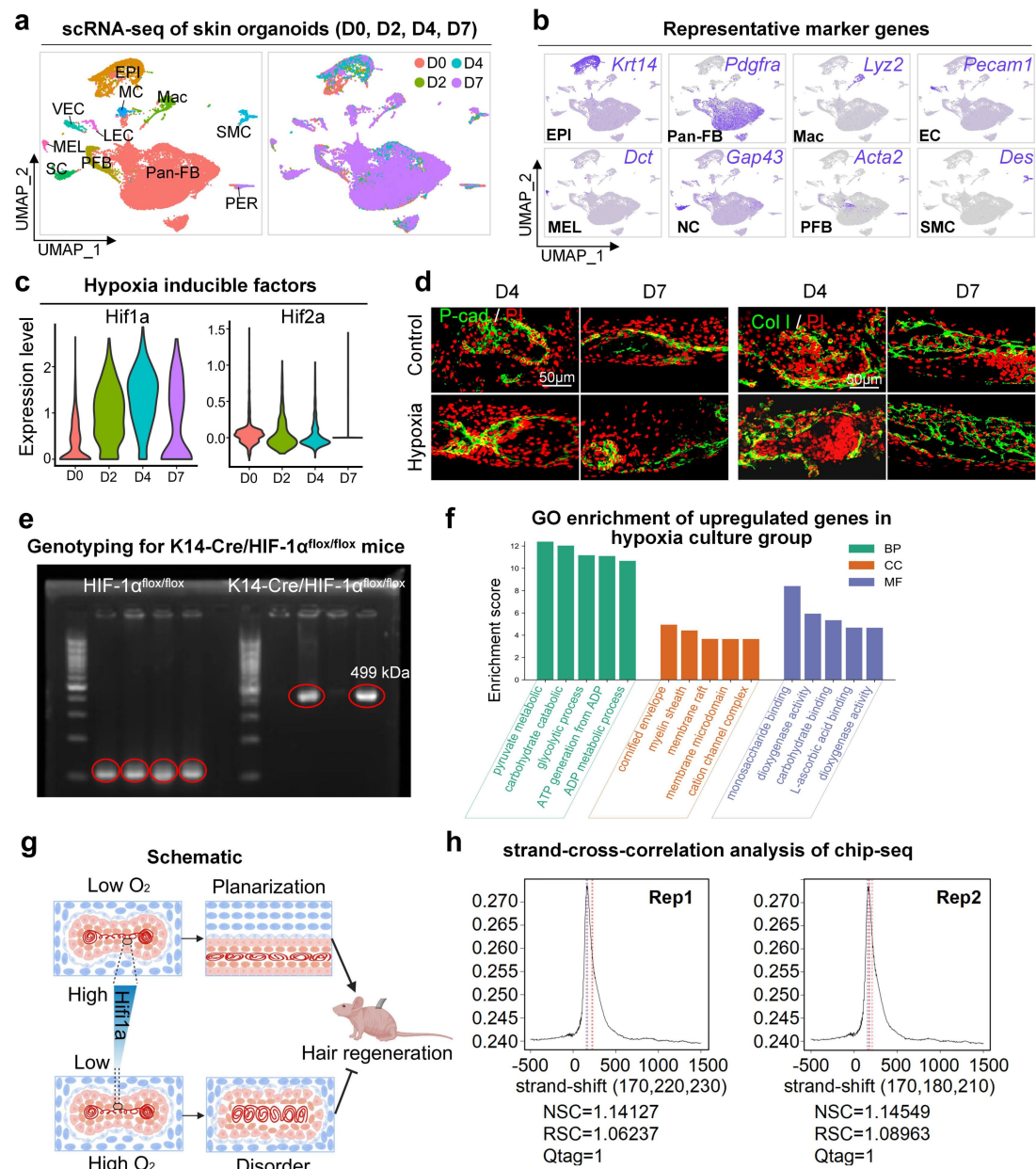
Extended Data Fig. 2



Extended Data Fig. 2: Multi-omics analyses show cellular and molecular changes during coalescence-planarization transition process

- a. UMAP plot displaying the dimensionality reduction clustering of D4 and D7 skin organoid samples.
- b. Bubble plot representing the marker genes for each cell cluster in the skin organoids (D4 and D7).
- c. List of Hif-1 pathway genes.
- d. Hif1a scores comparison across all cell clusters.
- e. Violin plot showing the scores of the hypoxia gene module in dermal and epidermal cell clusters
- f. The violin plot compares the hypoxia scores across subclusters of epidermal cells
- g. Violin plots showing the expression differences of Hif-1 pathway genes in D4 and D7 epidermal cells.

Extended Data Fig. 3



Extended Data Fig. 3: Hypoxia and Hif1a drive the planar skin formation

- a. UMAP clustering plot showing the integration of skin organoids at D0, D2, D4, and D7 time points with dimensionality reduction.
- b. Featureplot visualization of the expression of representative marker genes.
- c. Violin plots illustrating the expression trends of Hif1a and Epas1 (Hif2a) in the epidermal cell subsets at D0, D2, D4, and D7.
- d. The representative DNA electrophoresis bands illustrate the identification results of *K14^{cre}Hif1a^{flox/flox}*, with the red circle representing the Cre mouse.
- e. Representative immunofluorescence staining images of Col I and P-cad showing the phenotypic differences between 2% hypoxia culture and 21% normoxia culture of skin organoids.
- f. Bar chart displaying the enrichment of GO terms (BP, CC, and MF) for the upregulated genes in the 2% hypoxia culture.
- g. Schematic diagram showing hypoxia promoting planarization and hair regeneration of the skin organoid.
- h. Pearson cross-correlation analysis of Hif1a ChIP-seq data.

a Differential metabolites

b VIP score of differential metabolites

c Glycolysis gene sets

Glycolysis gene sets			
<i>Akt1</i>	<i>Aldoat2</i>	<i>Rps6kb2</i>	<i>Mknk2</i>
<i>Aldoc</i>	<i>Slc2a1</i>	<i>Eno1</i>	<i>ErbB2</i>
<i>Cdkn1a</i>	<i>Pfkfb</i>	<i>Hmox1</i>	<i>Trf</i>
<i>Pfkfb</i>	<i>Hk1</i>	<i>Aldoa</i>	<i>Angpt4</i>
<i>Cybb</i>	<i>Aldoat1</i>	<i>Hk2</i>	<i>Egln1</i>
<i>Pfkfb</i>	<i>Pdk1</i>	<i>Egln3</i>	<i>Plcg2</i>

d AUCell's Distribution

e qRT-PCR of glycolysis genes

f Lactate content

g Biological process (Hif1a+ vs Hif1a-)

h Glycolytic process-involved genes

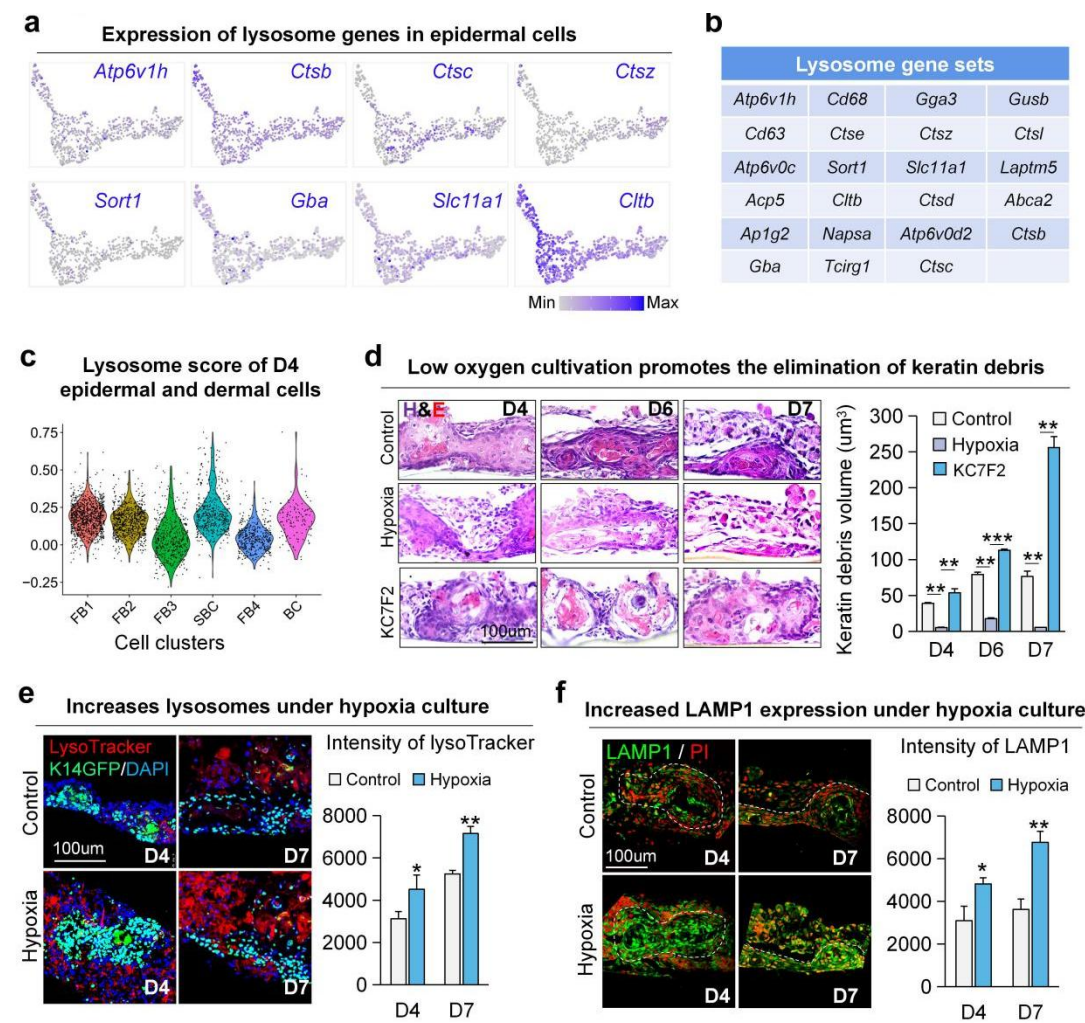
i Glycolysis or gluconeogenesis pathway

j

Extended Data Fig. 4: Glycolytic metabolism facilitates epidermal-dermal phase separation

- a. Differential metabolite heatmap depicting variations between D4 and D7 skin organoids, with 7 replicates per group.
- b. Bubble plot comparing Variable Importance in Projection (VIP) scores of differential metabolites in D4 and D7 organoids.
- c. AUC gene set used for glycolysis scoring.
- d. Glycolysis scores for all cell subpopulations.
- e. qPCR validation of gene expression changes in glycolysis-related genes during D4 and D7 organoid cultivation.
- f. Quantitative analysis of lactate levels. Left: Differential lactate levels (D7 vs D4) analyzed through metabolomics. Right: Differential lactate levels using a lactate assay kit.
- g. Functional enrichment analysis of upregulated genes in Hif1a-positive cells, focusing on Gene Ontology (GO) biological processes.
- h. Upper: RNA sequencing reveals the expression changes of Pkm, Ldha, Pgk1, and Mif during skin organoid self-organization process. Lower: Co-localization of Pkm, Ldha, Pgk1, and Mif with the epidermis and Hif1a.
- i. Glycolysis and gluconeogenesis pathways, with upregulated genes highlighted in red boxes and metabolites in green circles.
- j. Representative immunofluorescence images of GPI1, LDHA, PGK1, and PFKL during skin organoid self-organization process.

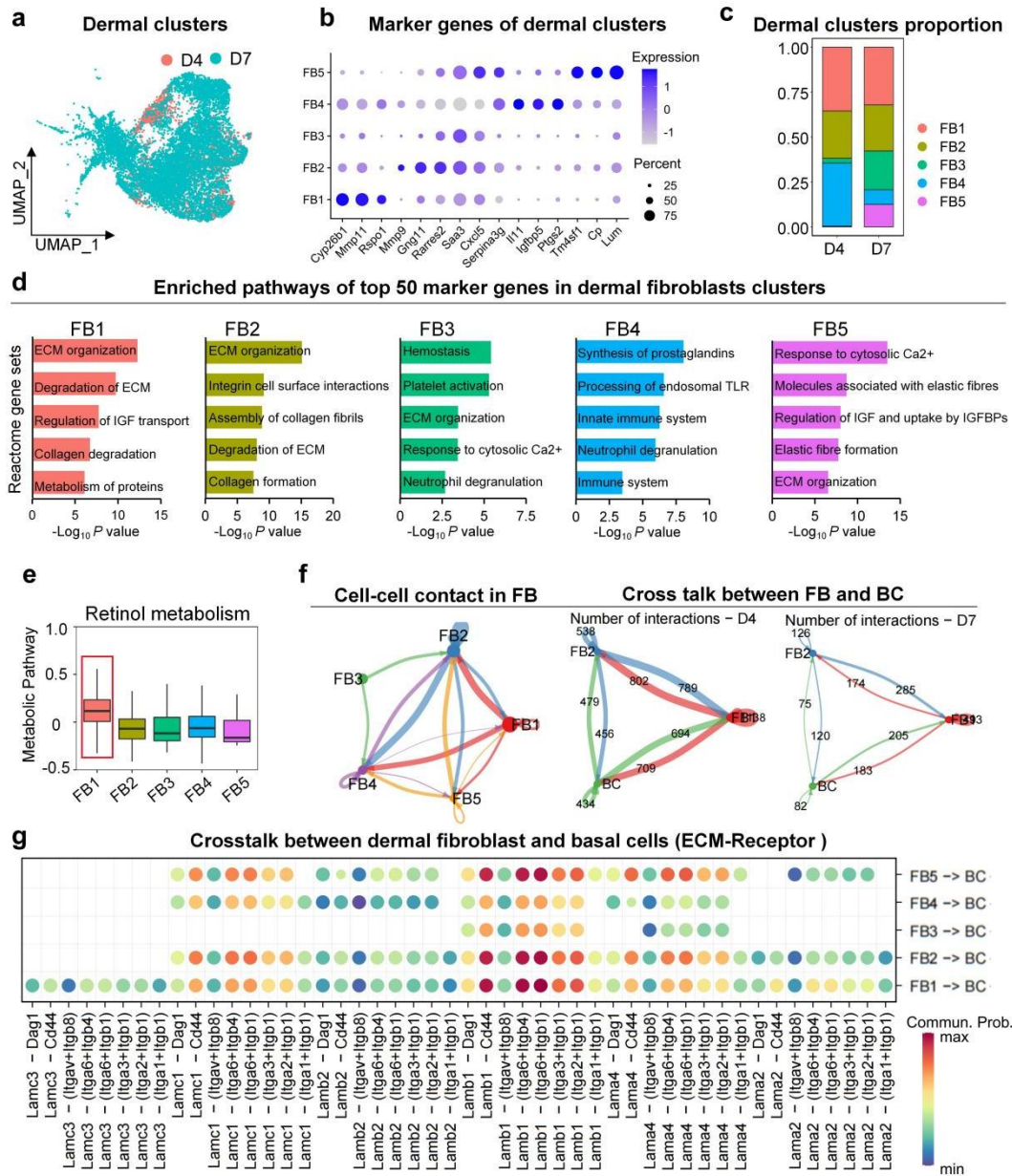
Extended Data Fig. 5



Extended Data Fig. 5: Hypoxia-driven lysosomal hydrolases clear keratin debris

- a. UMAP featureplot showing representative expression of lysosomal genes in the epidermal cell population. The lysosome gene set was used for AUC scoring.
- b. Lysosome gene set used for AUC scoring.
- c. Violin plot comparing AUC scores of lysosome genes between dermal and epidermal cell populations.
- d. Left: HE staining images demonstrating the changes in keratin fragments in skin organoids following KCF72 treatment or hypoxic culture. Right: Quantitative analysis of keratin debris levels.
- e. Left: LysosomeTracker staining showing changes in lysosome quantity in skin organoids following hypoxic culture. Right: Quantitative analysis of lysosomal fluorescence intensity.
- f. Changes in expression of the lysosomal membrane protein LAMP1 in skin organoids following hypoxic culture. Left: Immunofluorescence staining. Right: Quantitative analysis of LAMP1 fluorescence intensity.

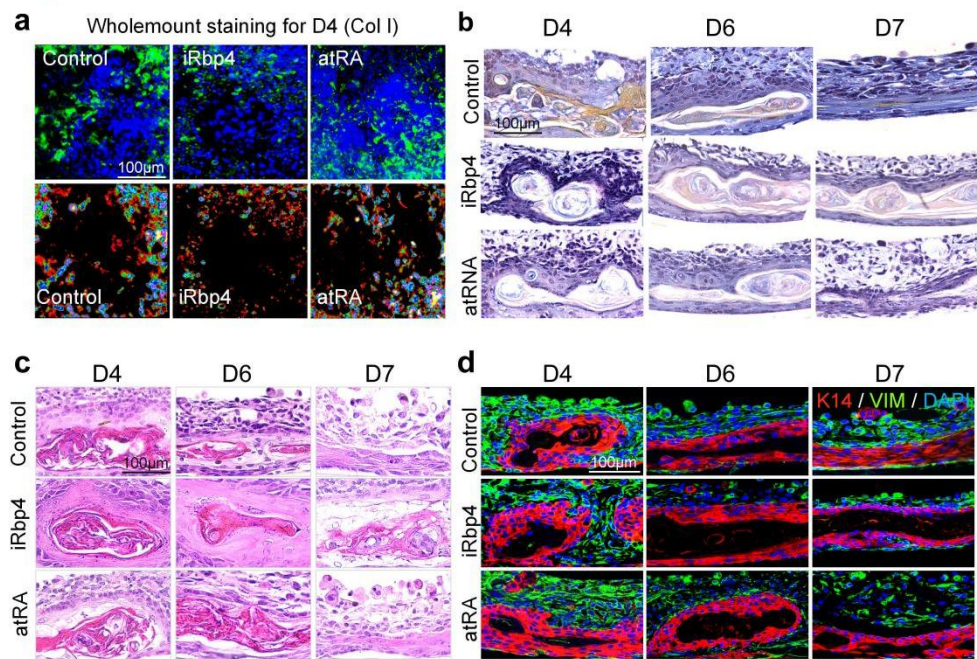
Extended Data Fig. 6



Extended Data Fig. 6: Metabolic heterogeneity in dermal fibroblasts

- a. UMAP plots showing the dimensionality reduction and clustering of D4 and D7 dermal fibroblasts.
- b. Marker genes defining subpopulations of dermal fibroblasts in skin organ.
- c. Percentage comparison of cell numbers in five dermal fibroblast clusters.
- d. Reactome functional enrichment analysis of the top 50 marker genes identified in the sub-clusters of dermal fibroblasts.
- e. The comparative analysis of retinol metabolism intensity among FB1-5 clusters by scMeabolism.
- f. Left: Cellchat analysis demonstrating the interplay among the five dermal fibroblast clusters; Right: Cell communication analysis revealing the interaction between FB1 and FB2 with epidermal basal cells.
- g. Crosstalk between dermal fibroblast and basal cells (ECM-Receptor).

Extended Data Fig. 7



Extended Data Fig. 7: Retinol metabolism supports self-organization of dermal fibroblasts and basal membrane formation

- a. Three-dimensional whole tissue staining to compare the expression of Col I of the iRBP4 group and atRA group at D4.
- b. Herovici staining to compare collagen neogenesis and the expression of keratin in iRBP4 group and atRA groups at D4, D6, and D7.
- c. HE staining to compare the expression of keratin in iRBP4 and atRA group at D4, D6, and D7.
- d. Immunofluorescence double staining to observe the epidermal planarization process in the iRBP4 group and atRA groups at D4, D6, and D7.

Supplementary Table

Supplementary Table 1: The antibody information used in immunostaining

Antibody	Company	Cat #
Bmp4	Beyotime	Cat # AF6312
Collagen I	Arigobio	Cat # ARG21965
Collagen III	Proteintech	Cat # 22734-1-AP
Collagen VI	Proteintech	Cat # 17023-1-AP
Collagen XVII	Beyotime	Cat # AF1078
Ctsl	Bioss	Cat # BS-1508R
Ctsd	Beyotime	Cat # AF1645
E-cadherin	Beyotime	Cat # AF0138
Eno1	Beyotime	Cat # AF5162
Fabp4	ABclonal	Cat # A0232
Gpi	Bioss	Cat # BS-10419R
HIF1A	Elabscience	Cat # E-AB-31662
KRT14	Boster	Cat # A01432
KLK7	Zenbio	Cat # 384788
Laminin	Abcam	Cat # ab11575
Lamp1	Beyotime	Cat # AF7353
Lamp2	Bioss	Cat # BS-2379R
Ldha	Affinity	Cat # DF6280
Mgp	Proteintech	Cat # 10734-1-AP
P63	GeneTex	Cat # GTX102425
P-Cadherin	R&D	Cat # AF761
Pgam1	Beyotime	Cat # AG2856
Pgk1	Beyotime	Cat # AF1825
Pfkl	Proteintech	Cat # 68385-1-Ig
DAPI	Beyotime	Cat # C1005
Rbp4	Proteintech	Cat # 11774-1-AP
SPP1	Beyotime	Cat # AF1651
Tenascin C	Beyotime	Cat # AF1651
Twist1	Zenbio	Cat # 507314
Vimentin	Beyotime	Cat # AF0318

Supplementary Table 2: The information of chemicals and recombinant proteins

	Company	Cat #
KC7F2	MCE	Cat # HY-P2230
2-DG	TargetMol	Cat # T24167
iENO1	TopSCIENCE	Cat # T0353
iPGAM1	Beyotime	Cat # ST1056
Paraformaldehyde (PFA)	Servicebio	Cat # G1101
Xylene	Chembk	Cat # 128686-03-3

PBS	Solarbio	Cat # P1010
Anhydrous ethanol	LMAI Bio	Cat # LM64-17-5
Trypsin	Gibco	Cat # R001100
RIPA	Beyotime	Cat # P0013B
DMEM/F12	Corning	Cat # 10092018

Supplementary Table 3: The information of primer for qPCR

Gene	Forward	Reverse
Abcg1	CTTTCCTACTCTGTACCCGAGG	CGGGGCATTCCATTGATAAGG
Aldh3b1	ATGGACTCGTTTGAAGACAAGC	GATGGCAATCTCAGACACCTC
Atp6ap1	GGCGGCAACAGTGGTATCTC	CACAGATTCCGGTCACTCGAC
Ctsc	CAACTGCACCTACCCTGATCT	TAAAATGCCCGGAATTGCCCA
Ctsd	GCTTCCGGTCTTTGACAACCT	CACCAAGCATTAGTTCTCCTCC
Ctsl	ATCAAACCTTTAGTGCAAGTGG	CTGTATTCCCCGTTGTGTAGC
Ctsz	GGCCAGACTTGCTACCATCC	ACACCGTTCACATTTCTCCAG
Eno1	TGCGTCCACTGGCATCTAC	CAGAGCAGGCGCAATAGTTTTA
Gpi1	TCAAGCTGCGCGAACTTTTTG	GGTTCTTGAGTAGTCCACCAG
Gys1	GAACGCAGTGCTTTTCGAGG	CCAGATAGTAGTTGTCACCCCAT
Hif1a	ACCTTCATCGGAAACTCCAAAG	CTGTTAGGCTGGGAAAAGTTAGG
Hif2a	CTGAGGAAGGAGAAATCCCGT	TGTGTCCGAAGGAAGCTGATG
Hk2	TGATCGCCTGCTTATTCACGG	AACCGCCTAGAAATCTCCAGA
Hk3	TGCTGCCCACATACGTGAG	GCCTGTCAGTGTTACCCACAA
Hmox1	AAGCCGAGAATGCTGAGTTCA	GCCGTGTAGATATGGTACAAGGA
Hmox1	AAGCCGAGAATGCTGAGTTCA	GCCGTGTAGATATGGTACAAGGA
Hsp90	AATTGCCAGTTAATGTCCTTGA	CGTCCGATGAATTGGAGATGAG
Lamp1	CAGCACTCTTTGAGGTGAAAAAC	ACGATCTGAGAACCATTTCGCA
Lamp2	TGTATTTGGCTAATGGCTCAGC	TATGGGCACAAGGAAGTTGTC
Ldha	TGTCTCCAGCAAAGACTACTGT	GACTGTACTTGACAATGTTGGGA
Ldhb	CATTGCGTCCGTTGCAGATG	GGAGGAACAAGCTCCCGTG
Pgk1	ATGTCGCTTTCCAACAAGCTG	GCTCCATTGTCCAAGCAGAAT
Rara	ATGTACGAGAGTGTGGAAGTCG	ACAGGCCCGGTTCTGGTTA
Rbp4	AGTCAAGGAGAACTTCGACAAGG	CAGAAAACCTCAGCGATGATGTTG
Rraga	CTCGGGCGCTGTTTTCTGA	CATGGCTGTATTGGGCATCAC
Rragc	AGATGTCACCCAATGAGACTCT	AGTCGTCCTGTGCATCAATGA
Tgfa	CACTCTGGGTACGTGGGTG	CACAGGTGATAATGAGGACAGC
Tpi1	CCAGGAAGTTCTTCGTTGGGG	CAAAGTCGATGTAAGCGGTGG